

# The Production and Application of Hydrogen in Steel Reheat Furnace Burners

Dara Safe

*Department of Mechanical Engineering, University of Wisconsin-Madison*

December 22, 2022

## Introduction

Rising greenhouse gas emissions from increased human activities involving fossil fuels are a global concern (Liu et al., 2021). The global steel sector is the second-largest industrial contributor to greenhouse gas emissions, with roughly eight percent of total carbon dioxide emissions from fossil fuels (Hasan Muslemani, 2021). One of the most energy-intensive processes within steelmaking is the steel reheating process, requiring 2.3 gigajoules per ton of steel, roughly 20% of the industry's total energy consumption (NREL, 1998). The UNFCCC's Paris Agreement declared to combat climate change globally in 2015 and has incentivized the steel industry to become carbon neutral by 2050 (Schmitz et al., 2021). This ambitious effort requires alternative fuels in industrial steel reheating to replace fossil fuels as the principal energy source. Hydrogen is considered one of the most promising solutions to achieve net zero carbon emissions partly due to the wide range of sourcing and high heating value (Liu et al., 2021). The following report starts with a background on the steel industry, current industrial reheat furnace technology, relevant methodology, and waste heat recovery methods. After the technical background, this paper evaluates renewable electricity and natural gas hydrogen production pathways to power reheat furnace burners to reduce carbon dioxide emissions. Finally, this report concludes with a recommendation of the most feasible route and considerations for future work.

## Overview of the Steelmaking Process

Primary steel production uses coke-based or direct reduced iron (DRI) steel production, as shown in Figure 1. 71% of steel today is processed using coke-based steelmaking (Association, 2022). The first stage of steelmaking involves reducing iron ore to pig iron in a blast furnace using coke as the reducing agent and limestone to remove impurities in the raw material. In the second stage, the pig iron's carbon content reduces from roughly 4.5% to 0.5% in a basic oxygen furnace, where carbon is removed by blowing oxygen gas and creating crude steel (Rackley, 2010). Next, the crude steel is cast into steel stock that can take the form of slabs, billets, or blooms. Finally, the casted steel undergoes a hot rolling process to shape the steel based on the end-use. The reheating furnace is an integral part of the rolling mill, as the steel must be heated before the recrystallization temperature for plastic deformation to occur.

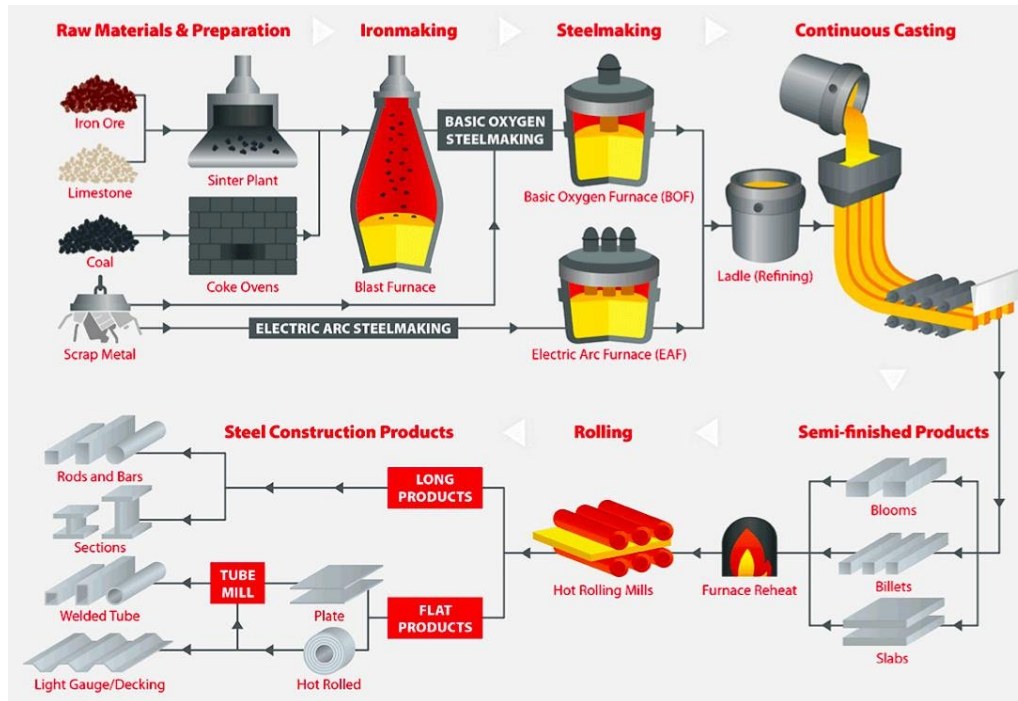


Figure 1: Overview of the steelmaking process reproduced from ("How Steel is Made")

Large quantities of useful by-product combustible gases are produced within the coke-based primary steel production route that is frequently used to power the reheating furnace. These include coke oven gas (COG) from coke production, blast furnace gas (BFG), and basic oxygen furnace gas (LDG). Most of the energy demands of reheating furnaces are satisfied by the valuable by-products mentioned as an efficient way to reduce natural gas dependence, thus reducing carbon footprint and fuel costs in reheating furnaces.

Table 1 shows the chemical compositions, heating values, and fuel volume production per ton of product for the respective process of the three combustible by-products. According to Caillat's paper on steel industry burners, the characteristics of these fuels tend to fluctuate depending on the production step and the raw material properties, like coal composition (Caillat, 2017). As a result, gas composition analyzers and mixing stations are used to fix the heating value or Wobbe index so that the combustion characteristics of the entire furnace are adjusted to maintain a constant air supply, as opposed to tuning each burner (Caillat, 2017).

Coke oven gas is rich in hydrogen and methane, thus containing a relatively high heating value at roughly half of the natural gas heating value. The heat content comes from the high concentrations of hydrogen and methane, which gives the fuel a high Wobbe index and usefulness as a standalone fuel for coke ovens, blast furnaces, and reheating furnaces.

The blast furnace gas heating value is low due to the high quantities of nitrogen and carbon dioxide, with the remaining content being carbon monoxide and little hydrogen (4%). The heating value is around a tenth of natural gas, which limits the fuel to low-temperature processes like steam generation and preheating the air in hot blast stoves. However, the fuel can be mixed with richer gases, such as coke oven gas or natural gas, before being used in high-temperature scenarios.

Basic oxygen furnace gas is created from the partial oxidation of carbon in the pig iron to high levels of carbon monoxide, between 60 -70%, which gives it a heating value of around a fourth of natural gas (Caillat, 2017). Due to the batch operation of the basic oxygen furnace, carbon monoxide

concentration and heating value are low during the beginning and end of the oxygen-blowing process, where the gas is typically flared (Joint Research et al., 2013). When the carbon monoxide levels are sufficiently high, the gas is cleaned and stored for valorization.

Table 1: Steel industry by-product combustible gas resources reproduced from (He & Wang, 2017)

	Chemical composition	Heat value	Production/t product
BFG	H: 4% CO: 25%, CO <sub>2</sub> : 20% The rest is N.	3000–3800/m <sup>3</sup>	1400–1800 m <sup>3</sup> /ton of iron
LDG	CO <sub>2</sub> : 15–20%, O <sub>2</sub> : ≤2.0%: CO: 60–70% N <sub>2</sub> : 10–20% H <sub>2</sub> ≤1.5%.	7500–8000 kJ/m <sup>3</sup>	80–100 m <sup>3</sup> /ton of liquid steel
COG	H <sub>2</sub> : 45–64%; CH <sub>4</sub> : 20–30%; CO: 5–10%; CO <sub>2</sub> : 2–5%; O <sub>2</sub> : 0.1–4%; C <sub>n</sub> H <sub>m</sub> : 0.1–3%.	16,000– 19,300 kJ/m <sup>3</sup>	400–450 m <sup>3</sup> /ton of coke

## Typical Industrial Reheat Furnace Description

The hot rolling process accounts for approximately 20% of an integrated steel plant's total energy consumption, and most of this energy is allocated to industrial steel reheat furnaces (Schmitz et al., 2021). Steel reheat furnaces heat the steel stock to high temperatures directly before hot rolling the steel into the final product. Generally, the steel is heated to a predetermined discharge temperature of around 1200°C in the reheat furnace and varies depending on the steel grade, the shape of the steel stock, and desired application of the steel (Schmitz et al., 2021). Industrial reheat furnaces are continuous systems where the steel stock is heated up to the desired discharge temperature as it travels through the furnace.

As illustrated in Figure 2, the steel slab travels in the x-direction through three distinct zones: the preheating, heating, and soaking zone. The steel stock enters an extended vestibule of the continuous furnace that preheats the load through counterflow combustion. The flue gas heat is recovered in this section to control the thermal stresses of the steel and allow for a more gradual increase in temperature. Next, the preheated steel enters the heating zone, where most heat absorption occurs. Lastly, the soaking zone controls the internal temperature of the steel to achieve a uniform temperature distribution throughout the steel stock.

Notably, the maximum heat transfer rate occurs within the heating zones and where the heating load is typically highest. Consequently, the heating zone is where the maximum difference in temperature along the slab thickness occurs (Li et al., 2020). Figure 3 shows the temperature distribution through the middle of the slab thickness as a function of time as the steel slab moves along a walker beam furnace with a residence time of 230 minutes to reach about 1200°C (Li et al., 2020).

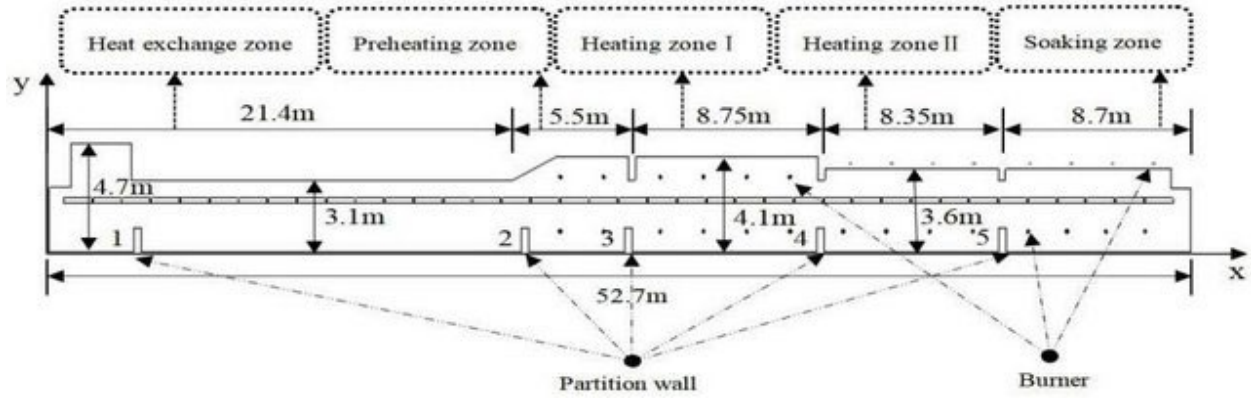


Figure 2: Dimensions and zones of a walking beam reheat furnace reproduced from (Li et al., 2020)

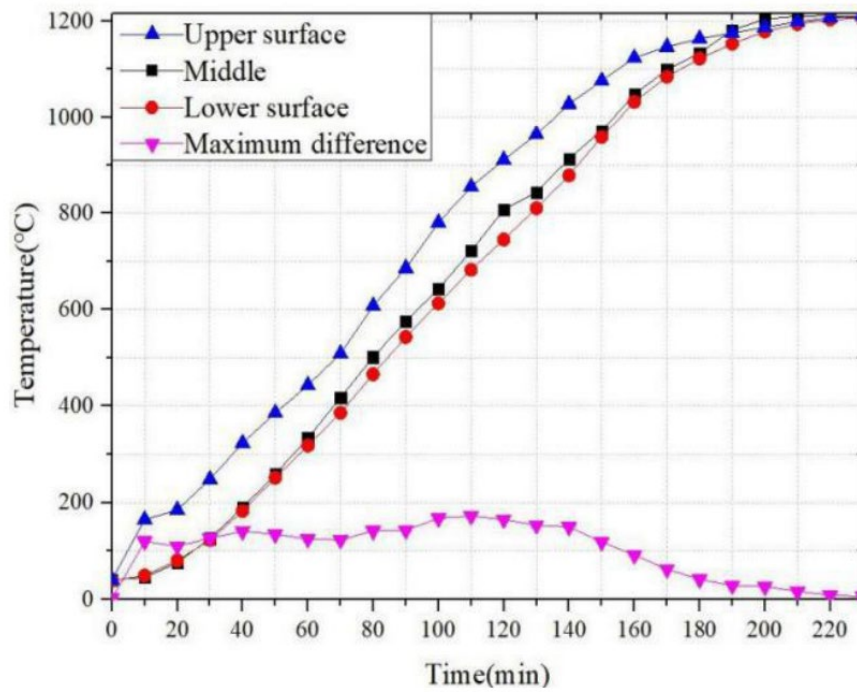


Figure 3: Temperature distribution of steel slab in a walking beam furnace with charge temperature of 1200 C and residence time of 230 minutes reproduced from (Li et al., 2020)

Typical high-capacity continuous reheating furnaces used for the mass production of steel are multi-zone walker beam and pusher-type furnaces. Pusher-type furnaces push cold steel stock forward along the hearth by pushers from the charging end of the furnace to the discharge end, as shown in Figure 4.

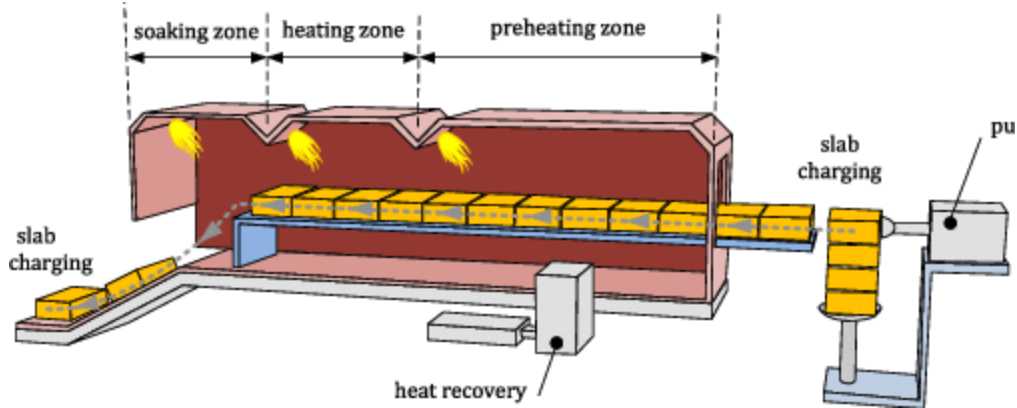


Figure 4: Pusher-type reheat furnace mechanism reproduced from (Feliu et al., 2014)

Walking beam furnaces are made up of water-cooled skids and refractory material to move the steel stock while voiding skid failure from high temperatures. As shown in Figure 5, the walking beam furnace has stationary beams where the steel stock rests and moving beams where the steel stock is lifted and moved forward to the next step along the furnace, where the moving beam resets to the original position.

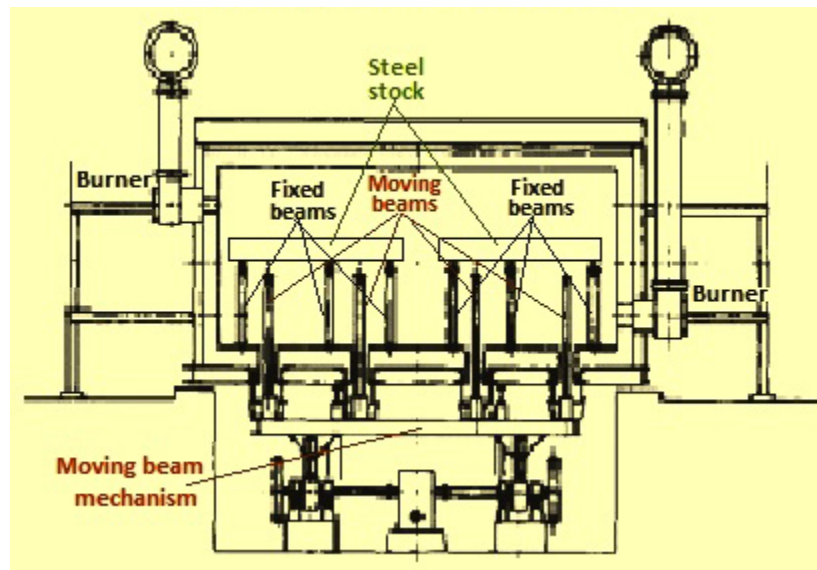


Figure 5: Walking beam furnace mechanism reproduced from (Satyendra, 2013)

Walker beam furnaces commonly incorporate cross-firing with side burners and radiant roof burners. Based on Figure 6, the recent development of industrial reheat furnaces has led to more extended preheating zones for better thermal efficiency in recent decades (Caillat, 2017). As mentioned previously, the preheating zone contains no burners. It utilizes convection from hot combustion off-gases to preheat the steel stock and simultaneously preheat the combustion air using leftover waste gas energy by utilizing regenerative or self-recuperative burners.


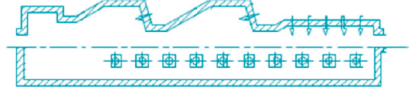
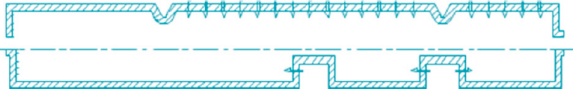


Years	Max length	Description	Schematic view
1970s	~35 m	Pusher furnace, frontal burners	
1975-80	~40 m	Walking beam furnace, frontal, lateral and roof burners	
1985-90	50/55 m	Walking beam furnace, frontal and roof burners	
1990-98	50/55 m	Walking beam furnace, lateral and roof burners	
Since 1995	~60 m	Walking beam furnace, lateral burners	

Figure 6: Types of industrial reheat furnaces over the recent past decades reproduced from (Caillat, 2017)

Due to the continuous flow of reheating to hot rolling, the reheat furnace size and output rate are directly related to the hot rolling mill capacity (Caillat, 2017). Reference industrial reheat furnace specifications are listed in Table 2. Notably, the furnace volume is roughly 1000 cubic meters and has a typical capacity of 160 tons of steel per hour, which feeds directly into the rolling mill (Schmitz et al., 2021). Industrial reheat furnaces contain several dozen burners for a total power output of roughly 50 megawatts (Caillat, 2017).

Table 2: Typical industrial reheat furnace specifications adapted from (Caillat, 2017; Schmitz et al., 2021)

Specification	Symbol	Value
Net capacity	$\dot{m}_{steel}$	160 t/hr
Effective dimensions	$L$	19.5 m
	$W$	14.8 m
	$H$	4.1 m
Furnace volume	$V_{furnace}$	1183.26 m <sup>3</sup>
Billet temperature	$T_{steel,in}$	20 °C
	$T_{steel,out}$	1250 °C
Total power output	$P_{furnace}$	50 MW
Power per burner	$P_{burner}$	~1MW

## Methodology

The energy consumption of industrial reheat furnaces is evaluated according to ISO 13579-1 methodology ("ISO 13579-1," 2013). Equation 1 represents the simplified energy balance for a reheat furnace under steady-state conditions where  $E_{fe}$  is the fuel equivalent energy which equates to the sum of various output energies. Other heat inputs are not included in the balance for the continuous steel reheating furnace system, such as the heat of combustion air. The outputs are expressed as the heat to steel  $h_{steel}$ , heat of off-gases  $h_{off-gas}$ , and other system losses  $q_{losses}$ .



$$E_{fe} = h_{steel} + h_{off-gas} + q_{losses} \quad (\text{Schmitz et al., 2021}) \quad (1)$$

Thermal efficiency  $\eta$  is characterized by the heat content of the steel  $h_{steel}$  divided by the energy provided by the fuel  $E_{fe}$  as defined in Equation 2.

$$\eta = \frac{\text{heat in steel stock}}{\text{heat in consumed fuel}} = \frac{h_{steel}}{E_{fe}} \quad (\text{Schmitz et al., 2021}) \quad (2)$$

The complete combustion of fuel in the furnace and minimal heat losses determines the most effective use of fuel. The typical thermal efficiency for state-of-the-art reheat furnaces is 57% (Schmitz et al., 2021).

According to Schmitz et al. at RWTH Aachen University, reheat furnace burners typically use an air-fuel ratio of 1.15 (Schmitz et al., 2021). The air-fuel ratio  $\lambda$  is the ratio of the actual amount of air supplied  $AFR$  to theoretical air needed for complete combustion  $(AFR)_{stoich}$  as depicted in Equation 3 (Schmitz et al., 2021).

$$\lambda = \frac{AFR}{(AFR)_{stoich}} \quad (\text{Schmitz et al., 2021}) \quad (3)$$

The desired air ratio in industrial reheat furnaces falls slightly higher than for complete combustion, where  $\lambda$  equals 1. It falls within the rational combustion regime where total heat loss is minimized, and thermal efficiency is maximized, as shown in Figure 7. Higher NO<sub>x</sub> emissions and heat loss due to excess air occur after the rational combustion regime, while black smoke formation and heat loss due to incomplete combustion occurs before.

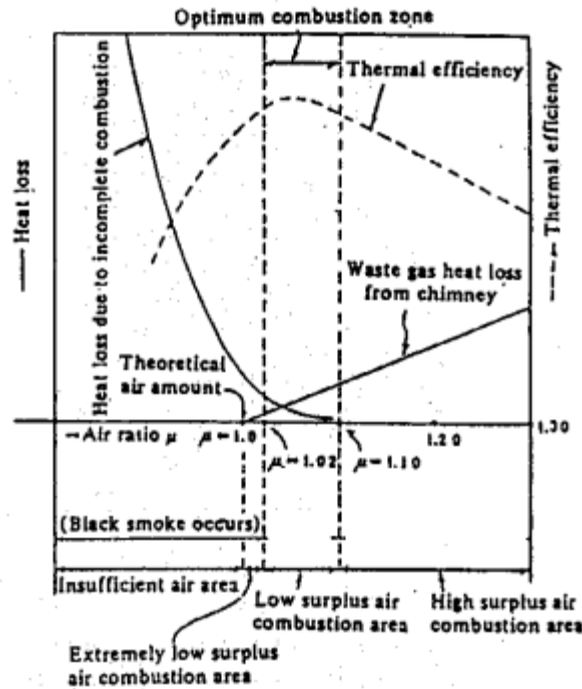


Figure 7: Relationship between air ratio and thermal efficiency (Energy Conservation in Steelmaking Industry)

Figure 8 illustrates the inputs and outputs associated with the furnace system. The system's inputs are the fuel energy and the sensible heat of combustion air, while the desired output is the heat absorbed by the steel. The most significant loss in the system is due to the flue gases, accounting for nearly 30% of energy loss at peak production rates (Si et al., 2011). Additional notable losses are wall losses caused by

the conduction of heat through walls in the furnace. Cooling water loss from lost energy when running cooling water along rollers, bearings, and doors to protect the furnace at extremely hot temperatures. Opening loss from the heat radiating to nearby colder surfaces or through furnace opening to surroundings. The unaccounted losses include heat storage loss, loss of furnace gases surrounding charging doors and furnace openings, incomplete combustion heat loss, and loss due to scale formation.

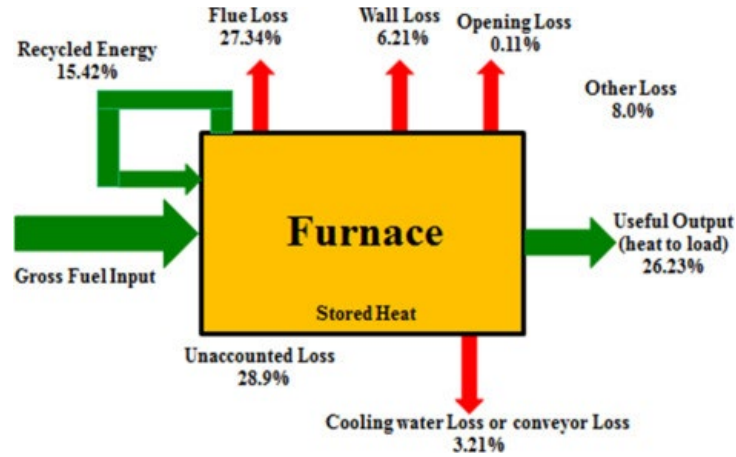


Figure 8: Schematic of industrial rehear furnace energy balance adapted from

## Gas Burner Characteristics

Standard fuels in rehear furnaces include natural gas and mixed steelmaking process gases, such as coke oven and blast furnace gas (Caillat, 2017). The gas burners can be external, internal, or semi-mixing types. The type of mixing is shown in Figure 9, and burner placement dictates the furnace heating characteristics and heat transfer efficiency. External mixing type burners mix the combustion air and fuel within the nozzle of the burner (Elkelawy & Mohamad, 2018). This burner configuration produces longer, lower-temperature flames, allowing for more uniform heat distribution (Elkelawy & Mohamad, 2018). Internal mixing types utilize premixing, where the combustion air and fuel are mixed before the start of combustion (Elkelawy & Mohamad, 2018). These types of burners typically form shorter, intense flames. The semi-mixing types are also known as partially mixed, producing flame characteristics between the external and internal mixing types and are considered helpful for flame stability (Elkelawy & Mohamad, 2018).

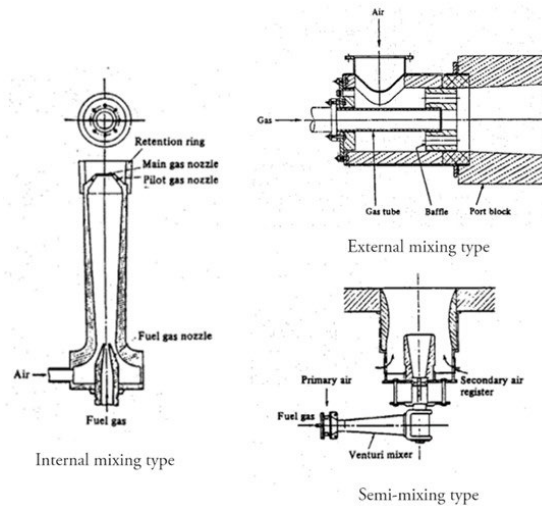


Figure 9: Gas burner mixing type designs (Energy Conservation in Steelmaking Industry)



The heating characteristics of the furnace are highly dependent on the arrangement of burners (García et al., 2019). Burners are classified into three types, axial-flow or frontal burners at the furnace nose sections, lateral burners at the side walls, and flat-flame radiant burners on the roof. Depending on the required temperature of the product, the flame produced by burners will have different geometries. For instance, axial-flow burners produce long and narrow flames, lateral burners create a variable or modulated flames, and roof burners create short and wide flames.

The axial-flow burners have high heating loads and produce long flames to drive convective heat transfer by recirculating combustions gases within the furnace. Axial flow burners facilitate temperature uniformity in the width direction while causing a temperature drop at the nose section in the longitudinal direction. Burners at the side wall are shorter variable flame burners that can produce long, transient, or modulated flames depending on the desired furnace heating characteristics. Roof or flat-flame burners charge the material by radiant heat transfer through the furnace's refractory lining and direct heat.

### Burner Waste Heat Recovery Methods

Burners are adapted to use waste heat as a secondary energy source through regenerative or self-recuperating design to reduce total fuel consumption and furnace efficiency (Reed, 1986). The waste heat is recovered for heat utilization and power generation to create electricity or mechanical energy (Reed, 1986). Furnace burners utilize heat by using hot exhaust gases to preheat the combustion air with a regenerative or self-recuperative model. Figure 10 illustrates the design of a self-recuperative burner model, which recycles the hot exhaust gases flowing in the furnace to transfer heat to the combustion air using counterflow heat exchange.

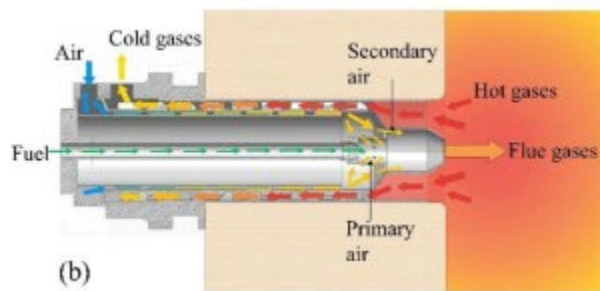


Figure 10: Self-recuperative burner application reproduced from (García et al., 2019)

Regenerative burners are composed of dual heat-recovering generators and heat-collecting reservoirs, typically filled with ceramic balls, to collect heat effectively (Climate, 2010). The regenerative burner is illustrated in Figure 11. According to Garcia et al., during the combustion of one side of the burner, the other is preheating the combustion air up to 1000 °C in the heat-recovery generator (García et al., 2019). The other burner then fires while the other now collects exhaust heat. The paper also mentions that heat regenerators can achieve energy savings of up to 48%. Furthermore, the self-recuperator is a cross-flow heat exchanger tube between the hot exhaust gases and combustion air to recover heat to the combustion air to preheat the combustion air up to 750 °C (García et al., 2019). Based on the literature, the exchanged heat systems improve combustion efficiency and save fuel demands by up to 30% (Fahim Muhammed, 2017; García et al., 2019).

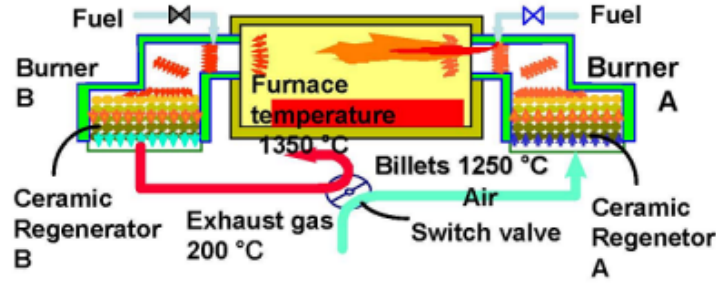


Figure 11: Regenerative burner application reproduced from (Climate, 2010)

## Application of Hydrogen as Fuel in Industrial Reheat Furnace

The use of hydrogen or hydrogen-rich gas as a fuel source in industrial reheat furnaces shows potential due to multiple benefits compared to the typically used blast furnace gas, basic oxygen furnace gas, coke oven gas, and natural gas. Considering that hydrogen is supplied at a competitive price to traditional fuels, increasing the concentration of hydrogen in existing furnaces can improve efficiency due to the higher heating values on a mass basis while significantly reducing carbon emissions (Mukherjee & Singh, 2021). Table 3 lists hydrogen's critical combustion property values compared to commonly used compounds in reheat furnace burners. The fuel properties dictate the burner operating parameters, such as fuel volumetric flow and air supply.

Table 3: Comparison of various fuel properties used in industrial reheat furnaces adapted from (ToolBox, 2018; von Scheele, 2021)

Specification	Hydrogen ( $H_2$ )	Methane ( $CH_4$ )	Carbon Monoxide ( $CO$ )
Density ( $kg/m^3$ )	0.08990	16.04	1.25
Adiabatic Flame Temperature ( $^{\circ}C$ )	2125	1942	2115
Lower Heating Value ( $kJ/m^3$ )	10758	35874	11570
Lower Heating Value ( $kJ/kg$ )	119664	50004	9252
Flame propagation velocity in Air ( $m/s$ )	2.83	0.45	0.52
Thermal diffusivity ( $cm^2/s$ ) at $20^{\circ}C$	0.756	0.21	0.208
Auto Ignition Temperature in Air ( $^{\circ}C$ )	572	632	608
Flammability Limits in Air (% volume)	4 – 74.2	5 – 15	12 – 75

Based on a case study by Mukherjee et al., increasing the hydrogen content in a hydrogen-methane fuel mixture from 10% to 90% results in a 2.2% increase in fuel efficiency when equating heat

input (Mukherjee & Singh, 2021). However, from a volumetric basis, the flow rate of the 90% hydrogen mixture must be roughly two and a half times that of the 10% hydrogen mixture flow rate to achieve equal heat inputs due to the considerably low density of hydrogen compared to methane (Mukherjee & Singh, 2021). Consequently, the gas piping system must be designed to accommodate the additional volumetric flow. A notable difference in the fuel properties is that the flame propagation speed of methane is about a sixth of the speed of hydrogen due to the low density, which makes the flame very hot and quick to spread, leading to safety concerns for flashback. Flashback is when the gas velocity becomes lower than the flame propagation velocity and causes the flame to travel backward into the burner. Burners must be able to accommodate flashbacks to avoid the risk of damaging the burners and potentially causing an explosion if the flame reaches the fuel supply (Vance et al., 2022). Equation 4 is the chemical formula for the combustion of hydrogen gas which requires two diatomic hydrogen molecules  $2H_2$  with a diatomic oxygen molecule  $O_2$  to form two molecules of water vapor  $2H_2O$  and released energy.



The flue gas in hydrogen is water vapor, unlike carbon dioxide in commonly used carbon-based fuels. This impacts the water concentration within the reheat furnace and raises questions regarding scale formation, decarburization, and temperature uniformity. Based on pilot tests run by Linde, a leading hydrogen distributor, there was no impact on steel quality when using hydrogen burners (Scheele, 2020a). Nevertheless, more concrete analysis is needed on the effect of hydrogen combustion on steel quality and furnace heating characteristics before considering hydrogen as a viable way to heat steel.

## Hydrogen Source and Production

Due to the increasing reliance on fossil fuels in the steel industry and the associated negative impact on global climate conditions, an incentive to utilize hydrogen has emerged. Typically, two routes are taken to create hydrogen: renewable sources and fossil fuels. According to Figure 12, approximately 50% of all hydrogen produced globally is from natural gas, while a small portion relies on renewable, or green, hydrogen (Liu et al., 2021). Green hydrogen production uses electrolysis, where water is broken down into its constituent parts, hydrogen and oxygen, using electricity from renewable sources, such as wind, solar, nuclear, etc. Then, the hydrogen is used as a fuel while the oxygen is released or used as an oxidizer for combustion. Fossil fuels, such as coke oven gas and natural gas, are commonly converted into hydrogen through reforming. The reforming process breaks down the long carbon chains in fossil fuels, which releases heat to create hydrogen. Hydrogen from fossil fuels is considered "blue" when capturing and storing carbon dioxide to reduce carbon emissions. When deciding which process is most feasible, the critical criteria are cost-effectiveness, purity of hydrogen, the ability for mass production, and total carbon emissions.

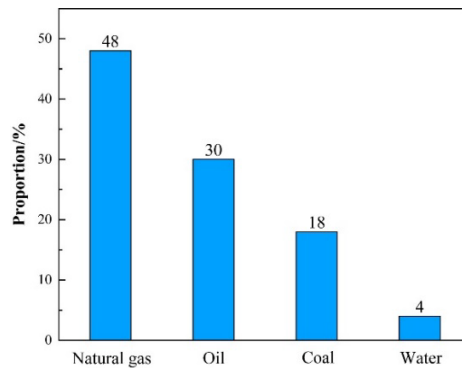


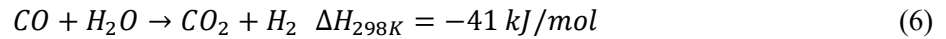
Figure 12: The percentage of raw materials for global hydrogen production reproduced from (Liu et al., 2021)

## Steam Methane Reforming and Carbon Capture

Natural gas reforming is the most dominant process for hydrogen production globally. Nearly half of the hydrogen produced in the world and 95% in the United States are made using this process (Liu et al., 2021; Office, 2022). The process converts methane, typically from natural gas, into hydrogen and carbon monoxide via a reaction with steam over a catalyst (Ji & Wang, 2021). The production process follows four steps shown in Figure 13. The natural gas is first purified to remove impurities and leave behind a pure form of methane. Next, methane reacts with steam at about 800°C to produce syngas, a mixture of carbon monoxide and hydrogen gas, shown in Equation 5.



Ji and Wang mention that the reaction in Equation 5 is significantly endothermic, which implies that external heat is required, typically provided by the combustion of natural gas (Ji & Wang, 2021). The following reaction is a water gas shift where the carbon monoxide reacts with steam over a metal-based catalyst, typically containing nickel or copper, depending on the temperature of the reaction, to convert into hydrogen and carbon dioxide, given in Equation 6 (NYSERDA, 2019).



The water gas shift reaction is carried out in two adiabatic stages, a high-temperature shift (HTS) at 350°C and a low-temperature shift (LTS) at 200°C stages (NYSERDA, 2019). Callaghan and Castro-Dominguez et al. explain the significant inverse relationship between the reaction equilibrium constant and temperature due to the reaction being slightly exothermic and concludes that carbon monoxide conversion into hydrogen increases at lower temperatures (Callaghan, 2006; Castro-Dominguez et al.).

Finally, the steam methane reforming gas mixture is purified using adsorption with carbon dioxide removal devices and undergoes methanation to remove leftover carbon oxides (NYSERDA, 2019).

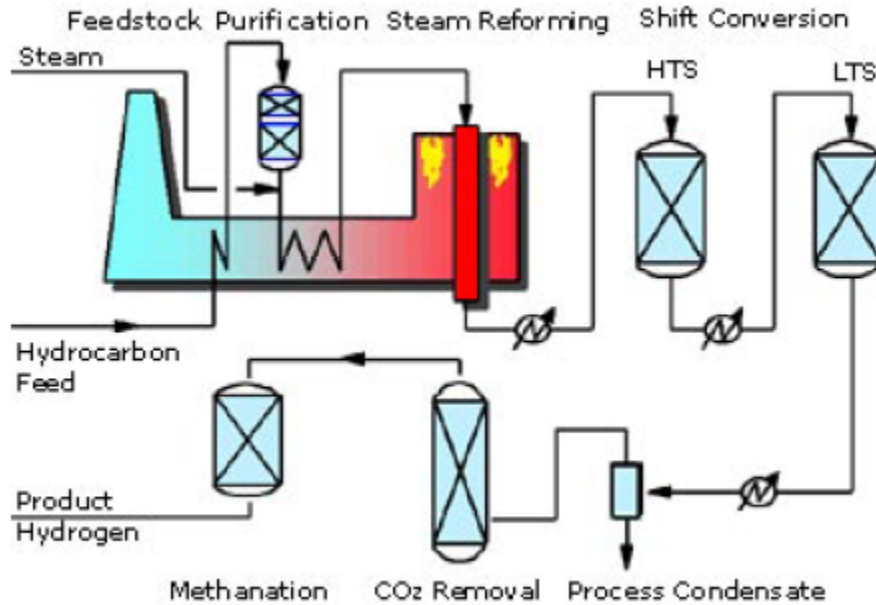


Figure 13: Steam methane reforming process reproduced from (NYSERDA, 2019)

According to Ji & Wang, the final composition of the gas is 70-75% hydrogen, 7-10% carbon monoxide, 6-14% carbon dioxide, and 2-6% methane (Ji & Wang, 2021). More advanced steam methane reforming plants utilize a two-stage pressure and vacuum swing adsorption (PSA/VSA) instead to purify the product to attain nearly pure hydrogen from the steam methane reforming gas and pure carbon dioxide from the tail gas (Shi et al., 2018). The difference between the two technologies is that vacuum swing adsorption uses a blower and vacuum pump to separate the atmospheric air, whereas pressure swing adsorption uses compressed air. From the findings of Liu et al., the first stage using PSA recovers 85% hydrogen and 90% carbon dioxide in the VSA apparatus (Liu et al., 2020). Soltani et al. point out that the typical steam methane reforming plant utilizing the processes described above emits 7 kilograms of carbon dioxide per kilogram of hydrogen, accounting for 3% of the global industrial sector emissions (Soltani et al., 2014). Despite steam methane reforming being a carbon-intensive process, carbon capture and sequestration (CCS) can mitigate most carbon dioxide emissions into the atmosphere (Soltani et al., 2014). According to Padro & Putsche, the two most common forms of sequestering are ocean disposal and underground injection (Padro & Putsche, 2010).

## Water Electrolysis

Water electrolysis is an electrochemical redox reaction involving an electric current to decompose water into hydrogen and oxygen (El-Emam & Özcan, 2019). The technology was founded in the 1800s to produce hydrogen, but due to more economical production alternatives such as steam methane reforming and coal gasification, there was a loss of interest (El-Emam & Özcan, 2019). It was not until the energy crisis of the 1970s that there was a stronger incentive to utilize this technology (El-Emam & Özcan, 2019). Water electrolysis is now used on a small scale and makes up 4% of global hydrogen demand. Electrolysis is classified into three methods, shown in Figure 14: alkaline electrolysis (AEL), proton exchange membrane (PEM), and solid oxide electrolysis (SOEC). The following briefly overviews the three proven technologies for large-scale hydrogen production.

Alkaline electrolysis and proton exchange membrane are the most developed water electrolysis technologies for commercial applications (Liu et al., 2021). AEL typically uses an electrolyte of liquid potassium hydroxide or sodium hydroxide. The hydroxide ions within the electrolyte are the charge carriers that transfer from the cathode to the anode to produce hydrogen gas. The diaphragm is used to separate the hydrogen and oxygen produced and is a critical component in ensuring the purity of the product by preventing gas bubble formation (El-Emam & Özcan, 2019). AEL has a working temperature of 70°C to 100°C and a pressure of 1 to 30 bars in large-scale applications (Rego de Vasconcelos & Lavoie, 2019). Rego de Vasconcelos & Lavoie explains AEL can also operate at high pressures up to 690 bar and are favorable for reducing the costs associated with the high-pressure requirements for transportation (Rego de Vasconcelos & Lavoie, 2019). Nevertheless, pressurized electrolysis has higher specific energy consumption at 56 to 60 kWh/kg  $H_2$  compared to large-scale ambient pressure electrolysis energy consumption of 48 to 60 kWh/kg  $H_2$  (Rego de Vasconcelos & Lavoie, 2019).

PEM pumps water to the anode, where the water molecule is separated into oxygen, hydrogen, and electrons (Ji & Wang, 2021). The hydrogen ions then migrate across a proton conducting membrane, made up of a highly acidic polymer called Nafion, to the cathode via direct current, where hydrogen gas is produced (El-Emam & Özcan, 2019; Rego de Vasconcelos & Lavoie, 2019). In commercial operation, PEM at a temperature below 150°C with high pressures of up to 400 bar (Rego de Vasconcelos & Lavoie, 2019).

SOEC is essentially the reverse reaction of PEM where steam at 700°C to 1000°C reacts with electrons at the cathode to produce hydrogen gas and oxygen ions (Rego de Vasconcelos & Lavoie, 2019). The oxygen ions then travel through the gas-tight membrane, forming the ions into gas and liberated electrons (Rego de Vasconcelos & Lavoie, 2019). The process is unique since it uses heat and

electricity to drive the breakdown of water molecules. Therefore, the heat provides part of the supplied energy, which lowers electricity demand and, consequently, the overall specific energy consumption to 28 to 39 kWh/kg  $H_2$  (Rego de Vasconcelos & Lavoie, 2019). Unlike the other technologies mentioned, SOEC is still in the prototyping stages, and further validation is required on cyclic stability, lifetime, and operation pressure before commercial use (Rego de Vasconcelos & Lavoie, 2019). Table 4 summarizes the operating conditions for each technology with corresponding measurements of specific energy consumption, as discussed in this section.

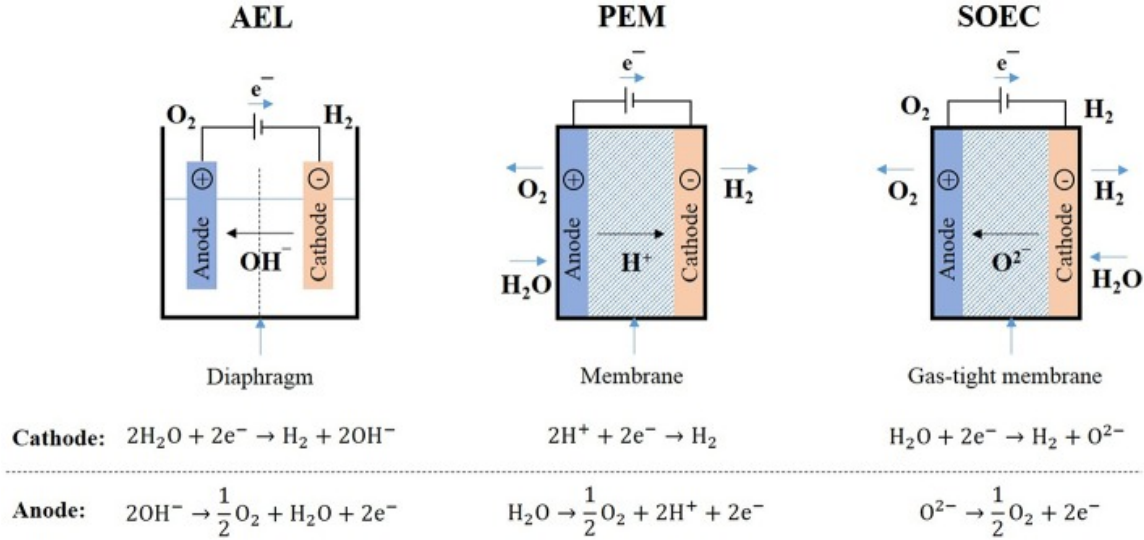


Figure 14: Methods for water electrolysis with respective anode and cathode reactions reproduced from (Rego de Vasconcelos & Lavoie, 2019)

Table 4: Operating conditions and development status of water electrolysis technologies adapted from (Dincer & Zamfirescu, 2016)

Technology		Development Status	T (°C)	P (bar)	SEC (kWh/kg $H_2$ )
AEL	Large scale	Commercial	70 - 90	1 - 25	48 - 60
	High-pressure	Commercial	70 - 90	Up to 690	56 - 60
PEM		Commercial	80 - 150	Up to 400	40 - 60
SOEC		Prototype	900 - 1000	Up to 30	28 - 39

## Comparison of Hydrogen Production Methods

In this paper, a brief overview of major hydrogen production processes has been presented. Hydrogen production methods can determine the cost-effectiveness, cleanness, and efficiency as a pathway for hydrogen production. The selection of the hydrogen production method will also depend on the scale of production and available energy resources. A comparative assessment of the considered hydrogen production methods is summarized in Table 5 and Table 6. Due to current trends to avoid fossil fuels, electrolysis technologies are assumed to be powered by renewable electricity, thus emitting roughly zero carbon emissions (Bartels et al., 2010). On the other hand, SMR alone involves a significant number of emissions. According to Ji and Wang, SMR has a global warming potential of 11.98 kg  $CO_2$  eq (Ji &



Wang, 2021). However, with the use of CCS the global warming potential reduces the global warming potential by 71.7% to 81.7%, depending on the efficiency of carbon dioxide sequestration (Ji & Wang, 2021). With CCS, SMR is considered quasi-clean shown in Table 5.

The efficiency of the process is critical in ensuring the overall viability of hydrogen as a fuel source for commercial applications. The developing electrolysis technology, SOEC, is known to have high energy efficiency due to the high process temperatures, which reduce the required voltage, hence lowering energy consumption (Chi & Yu, 2018). PEM is the next best in average efficiency and has the advantage of high power density and pressure within the fuel cell. Lastly, the most mature technology AEL is comparable to the efficiency of SMR, according to Table 5.

In electrolysis, the capital cost is typically related to the electrolyzer power capacity, operating strategy, and technology efficiency (Buttler & Spliethoff, 2018). Within electrolysis, AEL has favorable capital costs compared to PEM and SOEC. Notably, SMR alone is currently the cheapest in production cost and capital expenditure according to Table 5 and 6. Nevertheless, capital costs can nearly double when implementing CCS (Nikolaidis & Poullikkas, 2017).

Table 5: Cleanliness, efficiency, and capital expenditure for each hydrogen production technology adapted from (Dawood et al., 2020; IEA, 2022a; Ji & Wang, 2021)

	SMR	AEL	PEM	SOEC
*Cleanness (C/N/CCS)	N/CCS	C	C	C
Efficiency (%)	70 – 85%	62 – 82%	67 – 84%	75 – 90%
Capital Expenditure (CAPEX) (\$/kW)	500 - 900 900 -1600 (with CCS)	500 - 1400	1100 - 1800	2800 - 5600

\*Cleanness = clean with no emissions (C), non-clean with emissions (N), quasi-clean by using carbon capture and storage (CCS)

Table 6: Cost of hydrogen for each energy source adapted from (IEA, 2021, 2022b)

Energy Source	Cost (\$/kg $H_2$ )	
	2019	2050
Natural gas	0.5 – 1.7	
Natural gas with CCS	1 - 2	1.2 – 2.1
Renewable electricity	3 - 8	1.3 – 3.3

Natural gas costs vary from \$0.5 to \$1.7 per kilogram of hydrogen, depending on regional gas prices (IEA, 2021). Using CCS technology to reduce emissions increases the cost to \$1 to \$2 per kilogram of hydrogen (IEA, 2021). El-Emam and Özcan point out that the electrolytic hydrogen cost is strongly dependent on the mix of renewable energy being utilized to generate renewable electricity and the hydrogen generation plant capital costs, which explains the wide range of current hydrogen cost via renewable electricity (El-Emam & Özcan, 2019). Estimations from the International Energy Agency of hydrogen cost for the emerging hydrogen production routes are included in Table 6 (IEA, 2022b).

## Conclusion and Recommendation

Natural gas is one of the most viable pathways for introducing hydrogen as an energy carrier in reheat furnaces because it is commercially proven and is the least expensive feedstock for producing hydrogen in this analysis. However, CCS is required to address the high greenhouse gas emissions associated with using natural gas. According to the U.S. Department of Energy (DOE), the goal is to reduce the cost of distributed hydrogen production from renewable electricity to \$2 per kilogram of hydrogen by 2025 and \$1 per kilogram of hydrogen in the next decade (EERE, 2022). Based on the comparison section, the significant capital costs and lack of validation at a large scale make hydrogen via water electrolysis less feasible as an immediate solution for high carbon emissions in reheat furnaces (Rego de Vasconcelos & Lavoie, 2019). Significant research and development for electrolyzers and renewable electricity production efficiency are required to bring the cost of hydrogen using renewable sources to DOE targets.

In terms of hydrogen application in reheat furnaces, the unique combustion characteristics of hydrogen, such as high flame speed and adiabatic flame temperature, pose safety and operational challenges that must be considered before wide-scale integration (Baukal et al., 2021). Additionally, the design of burners in reheat furnaces should be modified to facilitate 100% hydrogen fuel concentration (Baukal et al., 2021). Despite industry leaders demonstrating the transition from carbon-based fuels to hydrogen in reheat furnaces on a small-scale, further validation is required (Scheele, 2020b).

It should be noted this paper neglects critical analysis of alternative hydrogen production, additional methods of reducing emissions in reheat furnaces, and others cost with hydrogen implementation. Emerging routes of hydrogen production using other forms of feedstock should be evaluated: biomass, coke oven gas, solar, oil, etc. (Hanley et al., 2018). Additionally, the use of thermal instead of electrical energy to power electrolysis seems promising since the cost of electricity is significantly higher than thermal energy, which gives incentive for further development of SOEC (El-Emam & Özcan, 2019). Not to mention, innovative combustion technology such as 'flameless' oxy-fuel combustion has had significant impacts on decreasing the reliance on fuel for heating in industrial reheat furnaces (Blasiak et al., 2007). Lastly, a thorough life cycle impact assessment is needed to evaluate missing information in this paper, such as production capacity, plant construction requirements, operational expenses, and fuel transportation costs (Cetinkaya et al., 2012).

## References

- References Association, W. C. (2022). *Coal & Steel*. Retrieved 11/21/2022 from <https://www.worldcoal.org/coal-facts/coal-steel/#:~:text=Steel%20is%20an%20essential%20material,in%20the%20steel%20making%20process.>
- Bartels, J. R., Pate, M. B., & Olson, N. K. (2010). An economic survey of hydrogen production from conventional and alternative energy sources. *International Journal of Hydrogen Energy*, 35(16), 8371-8384. <https://doi.org/https://doi.org/10.1016/j.ijhydene.2010.04.035>
- Baukal, C., Johnson, B., Haag, M., Theis, G., Henneke, M., Varner, V., & Wendel, K. (2021). *High Hydrogen Fuels in Fired Heaters*.
- Blasiak, W., Yang, W., Narayanan, K., & von Scheele, J. (2007). Flameless oxy-fuel combustion for fuel consumption and nitrogen oxides emissions reductions and productivity increase. *Journal of the Energy Institute*, 80, 3-11. <https://doi.org/10.1179/174602207X174379>
- Buttler, A., & Spliethoff, H. (2018). Current status of water electrolysis for energy storage, grid balancing and sector coupling via power-to-gas and power-to-liquids: A review. *Renewable and Sustainable Energy Reviews*, 82, 2440-2454. <https://doi.org/https://doi.org/10.1016/j.rser.2017.09.003>
- Caillat, S. (2017). Burners in the steel industry: utilization of by-product combustion gases in reheating furnaces and annealing lines. *Energy Procedia*, 120, 20-27. <https://doi.org/https://doi.org/10.1016/j.egypro.2017.07.152>
- Callaghan, C. A. (2006). Kinetics and Catalysis of the Water-Gas-Shift Reaction: A Microkinetic and Graph Theoretic Approach.
- Castro-Dominguez, B., Mardilovich, I. P., Ma, L. C., Ma, R., Dixon, A. G., Kazantzis, N. K., & Ma, Y. H. Integration of Methane Steam Reforming and Water Gas Shift Reaction in a Pd/Au/Pd-Based Catalytic Membrane Reactor for Process Intensification. LID - 10.3390/membranes6030044 [doi] LID - 44. (2077-0375 (Print)).
- Cetinkaya, E., Dincer, I., & Naterer, G. F. (2012). Life cycle assessment of various hydrogen production methods. *International Journal of Hydrogen Energy*, 37(3), 2071-2080. <https://doi.org/https://doi.org/10.1016/j.ijhydene.2011.10.064>
- Chi, J., & Yu, H. (2018). Water electrolysis based on renewable energy for hydrogen production. *Chinese Journal of Catalysis*, 39(3), 390-394. [https://doi.org/https://doi.org/10.1016/S1872-2067\(17\)62949-8](https://doi.org/https://doi.org/10.1016/S1872-2067(17)62949-8)
- Climate, A. P. P. f. C. D. a. (2010). The State-of-the-Art Clean Technologies (SOACT) for Steelmaking Handbook. In *Raw materials through steelmaking, including Recycling Technologies, Common Systems, and General Energy Saving Measures* (2nd ed., pp. 138).
- Dawood, F., Anda, M., & Shafiullah, G. M. (2020). Hydrogen production for energy: An overview. *International Journal of Hydrogen Energy*, 45(7), 3847-3869. <https://doi.org/https://doi.org/10.1016/j.ijhydene.2019.12.059>
- EERE. (2022). *Hydrogen Production*. Hydrogen and Fuel Cell Technologies Office. <https://www.energy.gov/eere/fuelcells/hydrogen-production>
- El-Emam, R. S., & Özcan, H. (2019). Comprehensive review on the techno-economics of sustainable large-scale clean hydrogen production. *Journal of Cleaner Production*, 220, 593-609. <https://doi.org/https://doi.org/10.1016/j.jclepro.2019.01.309>
- Elkelawy, M., & Mohamad, H. (2018). *Furnace Burner Design, Fluidization, Solids Handling and Processing*. <https://doi.org/10.13140/RG.2.2.25700.83849>

*Energy Conservation in Steelmaking Industry.*

- Fahim Muhammed , M. R., Noorshan. (2017). Energy Efficiency Analysis of an Industrial Reheating Furnaces and Investigating Efficiency Enhancing Opportunities : Literature Review. *International Journal of Engineering and Innovative Technology (IJEIT)*, Volume 6(Issue 6).  
<https://doi.org/DOI:10.17605/OSF.IO/2VPG8>
- Feliu, V., Rivas-Perez, R., & Castillo Garcia, F. J. (2014). *Robust fractional-order temperature control of a steel slab reheating furnace with large time delay uncertainty*.  
<https://doi.org/10.1109/ICFDA.2014.6967372>
- García, A. M., Colorado, A. F., Obando, J. E., Arrieta, C. E., & Amell, A. A. (2019). Effect of the burner position on an austenitizing process in a walking-beam type reheating furnace. *Applied Thermal Engineering*, 153, 633-645.  
<https://doi.org/https://doi.org/10.1016/j.applthermaleng.2019.02.116>
- Hanley, E. S., Deane, J. P., & Gallachóir, B. P. Ó. (2018). The role of hydrogen in low carbon energy futures—A review of existing perspectives. *Renewable and Sustainable Energy Reviews*, 82, 3027-3045. <https://doi.org/https://doi.org/10.1016/j.rser.2017.10.034>
- Hasan Muslemeni, A. H. M. A. X. L. A. K. K. A. F. A. A. J. W. (2021). Opportunities and challenges for decarbonizing steel production by creating markets for 'green steel' products. *Journal of cleaner production*, v. 315, pp. 128127--122021 v.128315.  
<https://doi.org/10.1016/j.jclepro.2021.128127>
- He, K., & Wang, L. (2017). A review of energy use and energy-efficient technologies for the iron and steel industry. *Renewable and Sustainable Energy Reviews*, 70, 1022-1039.  
<https://doi.org/https://doi.org/10.1016/j.rser.2016.12.007>
- How Steel is Made. In: StudyMeta.
- IEA. (2021). *Global Hydrogen Review 2021*. <https://www.iea.org/reports/global-hydrogen-review-2021>
- IEA. (2022a). *Electrolysers*. <https://www.iea.org/reports/electrolysers>
- IEA. (2022b). *Global average levelised cost of hydrogen production by energy source and technology, 2019 and 2050*. <https://www.iea.org/data-and-statistics/charts/global-average-levelised-cost-of-hydrogen-production-by-energy-source-and-technology-2019-and-2050>
- ISO 13579-1. (2013). In: International Organization of Standardization.
- Ji, M., & Wang, J. (2021). Review and comparison of various hydrogen production methods based on costs and life cycle impact assessment indicators. *International Journal of Hydrogen Energy*, 46(78), 38612-38635. <https://doi.org/https://doi.org/10.1016/j.ijhydene.2021.09.142>
- Joint Research, C., Institute for Prospective Technological, S., Remus, R., Roudier, S., Delgado Sancho, L., & Aguado-Monsonet, M. (2013). *Best available techniques (BAT) reference document for iron and steel production : industrial emissions Directive 2010/75/EU : integrated pollution prevention and control*. Publications Office. <https://doi.org/doi/10.2791/97469>
- Li, C., Huang, Y., Sun, J., Ni, Y., & Lu, L. (2020). Numerical simulation of pressure distribution in a walking-beam type reheating furnace. *IOP Conference Series: Earth and Environmental Science*, 467(1), 012025. <https://doi.org/10.1088/1755-1315/467/1/012025>
- Liu, B., Yu, X., Shi, W., Shen, Y., Zhang, D., & Tang, Z. (2020). Two-stage VSA/PSA for capturing carbon dioxide (CO<sub>2</sub>) and producing hydrogen (H<sub>2</sub>) from steam-methane reforming gas. *International Journal of Hydrogen Energy*, 45(46), 24870-24882.  
<https://doi.org/https://doi.org/10.1016/j.ijhydene.2020.06.264>
- Liu, W., Zuo, H., Wang, J., Xue, Q., Ren, B., & Yang, F. (2021). The production and application of hydrogen in steel industry. *International Journal of Hydrogen Energy*, 46(17), 10548-10569.  
<https://doi.org/https://doi.org/10.1016/j.ijhydene.2020.12.123>
- Mukherjee, R., & Singh, S. (2021). Evaluating hydrogen rich fuel gas firing. In. DigitalRefining: Engineers India Limited (EIL).

- Nikolaidis, P., & Poullikkas, A. (2017). A comparative overview of hydrogen production processes. *Renewable and Sustainable Energy Reviews*, 67, 597-611.  
<https://doi.org/https://doi.org/10.1016/j.rser.2016.09.044>
- NREL. (1998). *Steel Reheating for Further Processing*.
- NYSERDA. (2019). *Hydrogen Production - Steam Methane Reforming (SMR)*. N. Y. S. E. R. a. D. Authority.
- Office, U. S. H. a. F. C. T. (2022). *Hydrogen Production: Natural Gas Reforming*. U.S. Department of Energy Office of Fossil Energy and Carbon Management Retrieved from  
<https://www.energy.gov/eere/fuelcells/hydrogen-production-natural-gas-reforming>
- Padro, C., & Putsche, V. (2010). Survey of the Economics of Hydrogen Technologies.  
<https://doi.org/10.2172/12212>
- Rackley, S. A. (2010). Chapter 5 - Carbon Capture from Industrial Processes. In *Carbon Capture and Storage* (pp. 95-102). Butterworth-Heinemann. <https://doi.org/https://doi.org/10.1016/B978-1-85617-636-1.00005-5>
- Reed, R. J. (1986). *North American Combustion Handbook* (Third Edition ed., Vol. Volume 1: Combustion, Fuels, Stoichiometry, Heat Transfer, Fluid Flow).
- Rego de Vasconcelos, B., & Lavoie, J. M. (2019). Recent Advances in Power-to-X Technology for the Production of Fuels and Chemicals. (2296-2646 (Print)).
- Satyendra. (2013). *Reheating Furnaces and their Types*. <https://www.ispatguru.com/reheating-furnaces-in-steel-plants/#>
- Scheele, J. v. (2020a). Embracing hydrogen Flameless  
Oxyfuel for CO2  
-free heating. In.  
Scheele, J. v. (2020b). Embracing hydrogen Flameless  
Oxy-fuel for CO2 free heating. In.
- Schmitz, N., Sankowski, L., Kaiser, F., Schwotzer, C., Echterhof, T., & Pfeifer, H. (2021). Towards CO2-neutral process heat generation for continuous reheating furnaces in steel hot rolling mills – A case study. *Energy*, 224, 120155. <https://doi.org/https://doi.org/10.1016/j.energy.2021.120155>
- Shi, W., Yang, H., Shen, Y., Fu, Q., Zhang, D., & Fu, B. (2018). Two-stage PSA/VSA to produce H2 with CO2 capture via steam methane reforming (SMR). *International Journal of Hydrogen Energy*, 43(41), 19057-19074. <https://doi.org/https://doi.org/10.1016/j.ijhydene.2018.08.077>
- Si, M., Thompson, S., & Calder, K. (2011). Energy efficiency assessment by process heating assessment and survey tool (PHAST) and feasibility analysis of waste heat recovery in the reheat furnace at a steel company. *Renewable and Sustainable Energy Reviews*, 15(6), 2904-2908.  
<https://doi.org/https://doi.org/10.1016/j.rser.2011.02.035>
- Soltani, R., Rosen, M. A., & Dincer, I. (2014). Assessment of CO2 capture options from various points in steam methane reforming for hydrogen production. *International Journal of Hydrogen Energy*, 39(35), 20266-20275. <https://doi.org/https://doi.org/10.1016/j.ijhydene.2014.09.161>
- ToolBox, E. (2018). *Air - Diffusion Coefficients of Gases in Excess of Air*.  
[https://www.engineeringtoolbox.com/air-diffusion-coefficient-gas-mixture-temperature-d\\_2010.html](https://www.engineeringtoolbox.com/air-diffusion-coefficient-gas-mixture-temperature-d_2010.html)
- Vance, F. H., Goey, P., & van Oijen, J. (2022). Development of a flashback correlation for burner-stabilized hydrogen-air premixed flames. *Combustion and Flame*, 243, 112045.  
<https://doi.org/10.1016/j.combustflame.2022.112045>
- von Scheele, J. (2021). *Decarbonisation and Use of Hydrogen in Reheat Furnaces*.